the virus to mouse brain (*9*) was unsuccessful.

Conjunctival scrapings from nine other, similar infants with inclusion conjunctivitis treated in an identical manner failed to yield virus. This fact, and the high number of egg passages required for demonstration of viral activity in the one infant yielding virus (five, six, and seven passages on three attempts) suggest that of the vast number of virus particles seen microscopically in conjunctival smears only a minute proportion was able to propagate in eggs. During the period of these isolation attempts trachoma viruses proliferated readily in eggs from the same source. Thus, seasonal insusceptibility of eggs (*7*) is not a likely explanation for the failure of virus isolation in nine out of ten patients.

Undoubtedly the mother's genital tract is the source of the newborn's infection with inclusion conjunctivitis (*3*). The mother of our patient had marked vaginal discharge late in pregnancy, and examination 10 weeks after delivery indicated resolving cervicitis. However, cervical scrapings yielded no epithelial inclusions, and gross bacterial contamination vitiated attempts at virus isolation.

Whereas trachoma regularly involves the cornea and, if untreated, tends to produce progressive eye-tissue changes, inclusion conjunctivitis in newborn or adult does neither. We are currently comparing strains of trachoma virus (*7*) with the strain of inclusion conjunctivitis virus, in the hope of demonstrating some biological difference which might parallel the evident differences in the diseases caused by these agents.

L. Hanna, J. Zichosch, E. Jawetz, D. G. Vaughan, Jr., P. Thygeson
Department of Microbiology and *F. I. Proctor Foundation for Research in Ophthalmology, University of California Medical Center, San Francisco*

References and Notes

1. K. Stargardt, *Arch. Ophthalmol., Graefe's* **69**, 524 (1909); L. Schmeichler, *Berlin. klin. Wochschr.* **46**, 2055 (1909).
2. L. Halberstaedter and S. von Prowazek, *Berlin. klin. Wochschr.* **46**, 1839 (1909).
3. P. Thygeson, *Am. J. Ophthalmol.* **17**, 1019 (1934).
4. F. F. T'ang, H. L. Chang, Y. T. Huang, K. C. Wang, *Chinese Med. J.* **75**, 429 (1957).
5. B. R. Jones, L. H. Collier, C. H. Smith, *Lancet* **1**, 902 (1959).
6. L. Hanna, P. Thygeson, E. Jawetz, C. Dawson, *Science* **130**, 1339 (1959).
7. L. Hanna, E. Jawetz, P. Thygeson, C. Dawson, *Proc. Soc. Exptl. Biol. Med.* **104**, 142 (1960).
8. This work was supported in part by grants from the National Institutes of Health (B 604), the Burroughs Wellcome Fund, and the Research Committee of the University of California.
9. W. E. Hurst and P. Reeve, *Nature* **186**, 336 (1960).

1 August 1960

Performance Record of a Parthenogenetic Turkey Male

Abstract. A Beltsville Small White turkey poult of parthenogenetic origin hatched in the spring of 1958, matured, and produced semen containing viable spermatozoa. Semen from this male was used in January 1959 to inseminate seven virgin and seven previously mated Beltsville Small White turkey hens. Three hundred and twenty eggs were incubated, of which 175 or 54.7 percent were infertile. One hundred and twenty-two poults, about equally divided as to sex, hatched unaided from 145 fertile eggs.

During 1958 more than 8000 unfertilized eggs from 214 Beltsville Small White turkey hens were incubated, and data were collected on the incidence of parthenogenetic development. Seven hundred and twenty-two of these eggs (9.0 percent) were found to contain embryos of various ages, including 20 which survived to 29 days of incubation and were helped from the shell. One of three parthenogenetic poults raised to maturity produced usable quantities of semen containing viable spermatozoa. Semen from this parthenogenetic male was used in January 1959 to inseminate 14 Beltsville Small White hens, seven of which were young, unselected virgins. The other seven hens from the parthenogenetic line had been mated 8 months prior to these tests. Eggs laid by these 14 hens were identified as to hen number and subsequently incubated to obtain data on fertility and hatchability.

Data presented in Table 1 show that infertility was generally higher than would be expected for eggs from regular matings of Beltsville Small White turkeys, amounting to 50.3 percent of total eggs for the virgins and 61.1 percent for previously mated hens. Hatchability, when calculated on the basis of fertile eggs, was satisfactory, amounting to 85.1 percent for the virgins and 82.4 percent for eggs of previously mated hens. These percentages are within the range of normal variation for eggs of mated flocks of these turkeys.

Early embryonic mortality, 8.5 percent for virgins and 13.7 percent for previously mated hens, was generally higher than that for unhatched eggs from normal flocks of Beltsville Small White turkeys. The percentages of late mortality—6.4 percent for virgins, 3.9 percent for previously mated hens—may be considered normal, certainly no higher than normal. Late embryonic mortality in eggs from regular matings is generally two or three times greater than that occurring during the first 7 days of incubation.

One hundred and twenty-two poults were hatched from the 147 fertile eggs produced by the 14 hens. These poults were relatively free of major anatomical defects and thus were able to hatch unaided. They were about equally divided with respect to numbers of males and females. Poults were hatched from eggs laid as many as 44 days previously, and fertile eggs were obtained for as long a time as 50 days following a single insemination. The duration of fertility on the part of the sperm of the parthenogenetic male compares favorably with duration of fertility in normal turkeys as given in previously published figures.

Table 1. Incubation record of eggs produced by 14 Beltsville Small White turkey hens after insemination with semen from a parthenogenetic male.

Item	Virgins		Previously mated	
	No.	%	No.	%
Hens inseminated	7		7	
Eggs laid following insemination	189		131	
Fertile eggs	94	49.7*	51	38.9*
Dead embryos (1–14 days)	8	8.5	7	13.7
Dead embryos (15–28 days)	6	6.4	2	3.9
Poults hatched	80	85.1	42	82.4

* Percentage based on total eggs (the other percentages are based on fertile eggs).

M. W. Olsen
Animal Husbandry Research Division, Agricultural Research Center, Beltsville, Maryland

12 August 1960

Thermodynamic Treatment of Radio-Tracer Movements across Biological Membranes

Abstract. The movements of radioactive tracers across living cell membranes are discussed on the basis of thermodynamics of irreversible processes. Krogh's equation describing the flux of a tracer as a function of time is derived, and the significance of the "permeability" constant is clarified.

It is well known that, when a living cell is immersed in a large volume of medium containing a radioactive tracer, the intracellular concentration of the tracer rises roughly exponentially with time. The final concentration of the tracer is determined, as is expected, by the ratio at which the nonradioactive species of the same chemical substance is distributed across the cell membrane. The time constant with which the intracellular tracer concentration rises is considered to be determined by the "permeability" of the membrane with respect to the substance (*1*). The purpose of this report is to treat this behavior of the tracer movement from the

standpoint of thermodynamics of irreversible processes (*2–4*).

The system under consideration consists of three phases: the external fluid medium, the phase of protoplasm, and the intervening membrane. The membrane is treated as being uniform throughout the entire cell surface; if the living cell membrane has a mosaic structure consisting of patches of different properties, the following argument can be applied to the individual patches. The membrane contains two kinds of mobile particles: metabolites and nonmetabolites. By metabolites we mean such particles as CO_2, H^+, and NH_4^+, which are formed or consumed in the cell interior as the result of the cell metabolism. The nonmetabolites are those which do not take part in metabolism or do so only as catalysts. In the resting (stationary) state of the cell, the net fluxes of the nonmetabolites vanish, while those for the metabolites remain finite. The temperature and the pressure are considered to be constant throughout the system.

We denote the electrochemical potential for the ith particle species at position x perpendicular to the surface in the membrane by μ_i:

$$\mu_i = RT \ln C_i + z_i F\varphi \qquad (1)$$

where R is the gas constant, T is the temperature, C_i is the activity of the ith particle at position x in the membrane, z_i is the charge of the ith particle, F is the Faraday constant, and φ is the electric potential at position x. In the stationary (but nonequilibrium) state, the relationship between the flux of the ith species, J_i, and the electrochemical potential is given (see *4*, Eq. 6) by

$$\frac{d\mu_i}{dx} = -\Sigma_j R_{ij} J_j \qquad (2)$$

where the summation (with respect to the subscript j) is limited to the metabolites.

We define a new quantity, W_i^0 (which may be called the metabolic potential in the stationary state) by

$$\frac{dW_i^0}{dx} \equiv \Sigma_j R_{ij} J_j \qquad (3)$$

Then the condition for the stationary state (Eq. 2) can be written as

$$\frac{d(\mu_i + W_i^0)}{dx} = 0 \qquad (4)$$

or, by integrating this expression from the outer surface of the membrane ($x = 0$) to the inner surface ($x = a$), as

$$RT \ln \frac{C_i(a)}{C_i(0)} + z_i F\,\Delta\varphi + \Delta W_i^0 = 0 \qquad (5)$$

where $\Delta\varphi$ and ΔW_i^0 are the differences of these quantities across the membrane. Obviously, W_i^0 is different for different particle species; this quantity is a measure of the deviation of individual species from the distribution in the equilibrium state characterized by $\Delta W_i^0 = 0$. Since the classical work of Osterhout and Stanley (*5*), it has been understood that the deviation of the ionic distribution across the cell membrane is caused by the flow of metabolites (see also *2*).

When a radioactive tracer of a nonmetabolite is introduced into the surrounding fluid medium there is a flow of this tracer into the cell interior. Since we do distinguish the radioactive species from the nonradioactive species, and since there is production of entropy in mixing of two distinguishable particle species, the tracer must be treated as a separate species which moves independently of its nonradioactive analog (see *6*). We denote the tracer by subscript α and its nonradioactive analog by subscript 1. Then, it is found that W_α^0 is equal to W_1^0 because the two species should have the same concentration ratio across the cell membrane in the stationary state.

We express the flux of the radioactive tracer J_α (see *4*, Eq. 1) in the following form:

$$J_\alpha = -\Omega_{\alpha\alpha}\frac{\partial\mu_\alpha}{\partial x} - \Sigma_i \Omega_{\alpha i}\frac{\partial\mu_i}{\partial x} \qquad (6)$$

where $\Omega_{\alpha i}$ are phenomenological coefficients (in summation, $i \neq \alpha$). The flux J_α, the electrochemical potential μ_α, and the phenomenological coefficients are functions of both x and t. We introduce a new quantity W_α by

$$\sum_i \frac{\Omega_{\alpha i}}{\Omega_{\alpha\alpha}}\frac{\partial\mu_i}{\partial x} = \frac{\partial W_\alpha}{\partial x} \qquad (7)$$

From Eqs. 6, 7, and 1 it follows that

$$J_\alpha = -\Omega_{\alpha\alpha}\frac{\partial(RT \ln C_\alpha + z_\alpha F\varphi + W_\alpha)}{\partial x} \qquad (8)$$

In the final, stationary state J_α vanishes; therefore W_α coincides with W_α^0.

When the flux of the tracer is quasi-stationary, J_α is nearly independent of x. Dividing Eq. 8 by $\Omega_{\alpha\alpha}$ and integrating both members with respect to x, we find that

$$\frac{J_\alpha}{L_{\alpha\alpha}} = -RT \ln \frac{C_\alpha(a)}{C_\alpha(0)} - z_\alpha F\Delta\varphi - \Delta W_\alpha \qquad (9)$$

where

$$\frac{1}{L_{\alpha\alpha}} = \int_0^a \frac{dx}{\Omega_{\alpha\alpha}} \qquad (10)$$

and ΔW_α is given by the difference $W_\alpha(a) - W_\alpha(0)$. We define Teorell's factor ξ (see *7*, p. 364) by

$$RT \ln\xi = -z_\alpha F\,\Delta\varphi - \Delta W_\alpha \qquad (11)$$

When this factor is introduced, Eq. 9 becomes

$$J_\alpha = -L_{\alpha\alpha} RT \ln \frac{C_\alpha(a)}{\xi C_\alpha(0)} \qquad (12)$$

We denote the surface area of the cell membrane by A and the volume by v. The internal concentration of the tracer $C_\alpha(a)$ is related to J_α by

$$AJ_\alpha = v\frac{dC_\alpha(a)}{dt} \qquad (13)$$

When the system is close to the final, stationary state, $C_\alpha(a) \approx \xi C_\alpha(0)$; therefore,

$$\ln \frac{C_\alpha(a)}{\xi C_\alpha(0)} \approx \frac{C_\alpha(a) - \xi C_\alpha(0)}{\frac{1}{2}\{C_\alpha(a) + \xi C_\alpha(0)\}} \qquad (14)$$

Substituting Eqs. 13 and 14 in Eq. 12, it is finally found that the time course of the internal concentration of the tracer is given by

$$\frac{dC_\alpha(a)}{dt} = P\{\xi C_\alpha(0) - C_\alpha(a)\} \qquad (15)$$

which is equivalent to Krogh's (*1*) equation with the "permeability" P given by

$$P = \frac{2L_{\alpha\alpha} RT}{C_\alpha(a) + \xi C_\alpha(0)} \qquad (16)$$

The time course of the internal concentration is exponential only when P is independent of t. In general, P may vary with time.

When the concentration of the tracer is so small that we can safely assume that the distribution of the normal constituents in the system remains nearly unaffected by the introduction of the tracer, a further simplification can be made. In this case, μ_i ($i \neq \alpha$) does not vary with time. Furthermore, the value of J_α measured at a given time after introduction of the tracer, which is a monotonic function of the amount of the tracer introduced, can be taken as proportional to the amount of the tracer. (In fact, the measured time constant of the tracer movement is independent of the amount of tracer used under ordinary experimental conditions.) Each of the coefficients $\Omega_{\alpha\alpha}$, Ω_{α_1}, Ω_{α_2}, . . . is then proportional to the local concentration of the tracer, and the ratios $\Omega_{\alpha i}/\Omega_{\alpha\alpha}$ in Eq. 7 are independent of t; hence, W_α depends only on x ($W_\alpha = W_\alpha^0$). When we replace $\Omega_{\alpha\alpha}$ with UC_α (U being the mobility) and $(z_\alpha F\varphi + W_\alpha)$ with $RT \ln \xi(x)$, Eq. 8 becomes

$$J_\alpha = -\frac{U}{\xi(x)}\frac{\partial[C_\alpha\xi(x)]}{\partial x} \qquad (17)$$

This equation can readily be converted, after integration, into the form of Eq. 15, with P given by the reciprocal of the integral of $\xi(x)/U$. Under these circumstances P is independent of time and can actually be taken as a measure of the "permeability" because the values of U and $\xi(x)$ for the tracer are nearly the same as those for its nonradioactive analog.

I. TASAKI

National Institutes of Health, Bethesda, Maryland

References

1. A. Krogh, *Proc. Roy. Soc.* (*London*) **B133**, 140 (1946).
2. I. Prigogine, *Introduction to Thermodynamics of Irreversible Processes* (Thomas, Springfield, 1955).
3. S. R. de Groot, *Thermodynamics of Irreversible Processes* (Interscience, New York, 1951).
4. J. G. Kirkwood, *Ion Transport Across Membranes*, H. T. Clarke, Ed. (Academic Press, New York, 1954).
5. W. J. V. Osterhout and W. M. Stanley, *J. Gen. Physiol.* **15**, 667 (1932).
6. L. H. Nims, *Yale J. Biol. and Med.* **31**, 373 (1959).
7. T. Teorell, *Progr. in Biophys. and Biophys. Chem.* **3**, 305 (1953).

28 July 1960

Light and Electron Microscope Study of Cell Walls of Brown and Red Algae

Abstract. A survey of the structure of the cell walls of green, brown, and red algae, as seen under light and electron microscopes is in progress. In this report a comparison of the cell wall structure of a brown alga, *Dictyota flabellata*, and a red alga, *Helminthocladia californica*, is presented. In *Dictyota*, typical of the brown algae, the microfibrillar pattern in the apical cells and in the adjacent cells of the thallus tip is reticulate. In mature cells the microfibrils are dominantly parallel in orientation. Pits, fields of closely set pores, are distinctive. The microfibrils in the pit areas are masked by nonfibrillar material. *Helminthocladia*, with a cell wall characteristic of the red algae, differs from *Dictyota* in that the microfibrillar pattern is reticulate throughout the thallus. In the pit areas the microfibrils are not masked by amorphous material.

Introductory electron microscope studies began with an examination of the cell wall of the green alga, *Valonia* (*1*). Later work on other species of the Chlorophyta demonstrated a great variability in the structure of the wall (*2*). On the basis of the crystalinity of cellulose, three classes were recognized in the group as a whole (*3*). Detailed electron microscope reports on cell wall structure in the brown and in the red algae are comparatively few; among them are the papers of Cronshaw *et al.* (*4*) and Myers *et al.* (*5*).

The specimens of brown and red algae were collected on the coast of southern California in tide pools of the littoral zone and also during skin-diving expeditions in the sublittoral zone to depths of 40 feet. In the present report the structure of the walls of the brown alga *Dictyota flabellata* and the red alga *Helminthocladia californica* is compared. The two species examined appear to be characteristic of their respective groups. So far as we are aware, they have not been previously described.

Dictyota flabellata, a member of the order Dictyotales (*6*), is a smooth-margined, dichotomously branched brown alga which grows attached to rocks in tide pools and to depths of about 40 feet (*7*). It is a low-growing Phaeophyte with blades up to 15 cm long, 3 cm wide, and approximately 150 μ thick. As is characteristic for the order, the blade possesses apical growth. In *Dictyota* a single lens-shaped apical cell with a thick outer wall cuts off one cell which then undergoes enlargement and anticlinal septation, forming rows of cells radiating from the apex (*6*). The mature blade, as seen in transverse section, is three cell layers thick. The upper and lower layers consist of cuboidal cells about 20 μ deep. The central layer consists of larger rectangular cells, about 100 μ long, 45 μ wide, and 80 μ deep. Intercellular spaces occur at the cell corners. In the large central cells, pit fields are visible under the light microscope on all cell faces where cell walls are in contact. Preliminary microchemical tests indicate that the cell wall consists of cellulose (I_2KI and H_2SO_4, 80 percent) and pectic materials (Ruthenium red).

For study under the electron microscope the first millimeter of the young blade tip, which includes the apical cell, was isolated by dissection and then cleared of noncellulose material by treatment in a 1:1 solution of 10 percent nitric acid and 10 percent chromic acid at a temperature of 20°C for 2 to 3 hours. After 6 to 10 washings in distilled water, the fragments were ultrasonically macerated at 1 Mcy/sec for 30 seconds. Drops of this suspension which yielded whole cells, cell fragments, and clumps of cells were then placed on Formvar-coated grids and shadowed with palladium.

In the walls of the apical cell and the adjacent cells of the growing tip, the microfibrillar pattern is reticulate. Pores, groups of pores, or pits (*8*) are evident in the loose microfibrillar network. In fragments where clearing is not complete, plasmodesmata are evident in pores and pits. Thickening of the cell wall is evident in the increasingly larger cells in the first 300 μ of the thallus tip. The microfibrils, ranging in diameter from 100 to 250 angstroms, are deposited in parallel orientation and effectively mask the primary reticulate wall pattern except in specialized pit field areas. In these areas the microfibrils are masked by nonfibrillar material (Fig. 1). In torn fragments of pit areas, however, the underlying microfibrils are visible.

Helminthocladia californica, a red alga, a member of the order Nemalionales (*6*), also occurs attached to rocks in upper intertidal pools (*7*). The mucilaginous thallus is irregularly and indeterminately branched and may reach a length of 15 cm. Under the light microscope the thallus is seen to be of multiaxial construction with a medulla of interwoven, septate, branched filaments, ranging from 5 to 25 μ in diameter, which terminate in an outer coating of filament tips forming the cortex. The filaments increase in

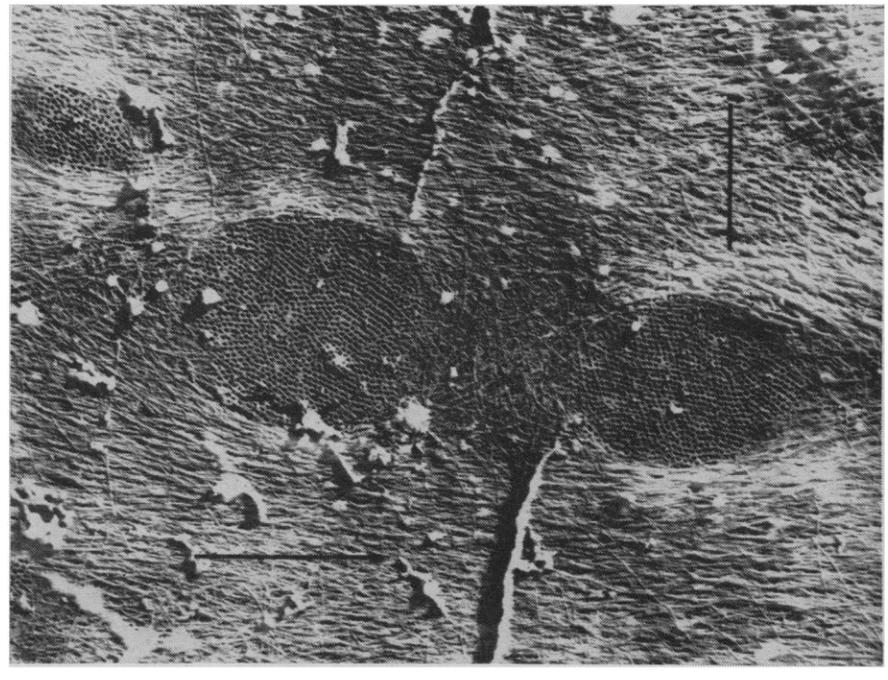

Fig. 1. Portion of the wall of a large central cell of *Dictyota flabellata.* Two large pits are flanked by microfibrils with a dominantly parallel orientation and are separated by an area in which the fibrils retain the reticulate pattern. The arrow indicates the axis of the cell wall. Scale, 2μ.